Signal Transduction

Molecular Cancer Research

HIF1α Regulates mTOR Signaling and Viability of Prostate Cancer Stem Cells

Maximilian Marhold[1], Erwin Tomasich[1], Ahmed El-Gazzar[1], Gerwin Heller[1], Andreas Spittler[2], Reinhard Horvat[3], Michael Krainer[1], and Peter Horak[1]

Abstract

Tumor-initiating subpopulations of cancer cells, also known as cancer stem cells (CSC), were recently identified and characterized in prostate cancer. A well-characterized murine model of prostate cancer was used to investigate the regulation of hypoxia-inducible factor 1α (HIF1A/HIF1α) in CSCs and a basal stem cell subpopulation ($Lin^-/Sca\text{-}1^+/CD49f^+$) was identified, in primary prostate tumors of mice, with elevated HIF1α expression. To further analyze the consequences of hypoxic upregulation on stem cell proliferation and HIF1α signaling, CSC subpopulations from murine TRAMP-C1 cells ($Sca\text{-}1^+/CD49f^+$) as well as from a human prostate cancer cell line ($CD44^+/CD49f^+$) were isolated and characterized. HIF1α levels and HIF target gene expression were elevated in hypoxic CSC-like cells, and upregulation of AKT occurred through a mechanism involving an mTOR/S6K/IRS-1 feedback loop. Interestingly, resistance of prostate CSCs to selective mTOR inhibitors was observed because of HIF1α upregulation. Thus, prostate CSCs show a hypoxic deactivation of a feedback inhibition of AKT signaling through IRS-1. In light of these results, we propose that deregulation of the PI3K/AKT/mTOR pathway through HIF1α is critical for CSC quiescence and maintenance by attenuating CSC metabolism and growth via mTOR and promoting survival by AKT signaling. We also propose that prostate CSCs can exhibit primary drug resistance to selective mTOR inhibitors.

Implications: This work contributes to a deeper understanding of hypoxic regulatory mechanisms in CSCs and will help devise novel therapies against prostate cancer. *Mol Cancer Res; 13(3); 556–64. ©2014 AACR.*

Introduction

On the basis of the cell-of-origin hypothesis, prostate cancer is one of the tumors known to harbor a distinct subpopulation of cancer stem (or initiating) cells (CSC), which are thought to confer resistance to common therapeutic measures, be it chemotherapy or radiotherapy (1, 2). The exact origin of prostate CSCs is widely discussed, as basal and luminal prostate epithelial cells are both capable of developing into prostate CSCs and play a role in tumorigenesis (3–8). On the basis of their expression of specific surface markers, several subsets of human prostate CSCs, either of basal or luminal origin, were identified (9–11). Prostate CSCs have also been isolated from the mouse prostate, based on the expression of integrin α6/CD49f and stem cell antigen 1 (Sca-1; refs. 12–14). The jury is still out on which of these models best represents human disease (15).

Recently, HIF1α has been shown to maintain the stemness of hematopoietic stem cells (HSC) in the hypoxic niche of the bone marrow (16). In parallel, it seems that prostate cancer cells target this HSC niche, leading to metastatic disease (17). Conversely, hypoxia leads to an increased metastatic potential of prostate cancer cells (18). Low oxygen levels, as present in the tumor microenvironment of solid tumors, result in the stabilization of the HIF1α protein by posttranslational mechanisms. HIF1α forms a heterodimeric transcriptional complex with HIF1β, translocates to the nucleus, and binds hypoxia-responsive elements found in the promoter regions of multiple downstream target genes, activating various adaptive pathways. Among many others, the PI3K/mTOR signaling pathway is regulated by hypoxic signaling (19). This pathway integrates growth factor signaling, cell metabolism, as well as diverse cellular stressors and modulates the adaptation of cell proliferation, apoptosis, autophagy, and protein translation (20) and has a central role in prostate carcinogenesis (21). mTOR functions as a nutrient/hypoxia sensor and controls protein synthesis by phosphorylation of its two main targets, p70-S6 kinase 1 (S6K1) and the eIF4E-binding protein 1 (4E-BP1). Its central role makes it a bona fide target for molecular therapy, and its inhibition has been shown to be effective in renal cell and breast cancer (22, 23).

We hypothesized that prostate CSCs may exhibit differential hypoxic signaling. Given the complex regulation of mTOR in hypoxia through multiple mechanisms and feedback loops, this might in turn affect their viability, stemness, and metastatic potential.

Materials and Methods

Cell culture and conditions

The DU145 and TRAMP-C1 cancer cell lines were obtained from ATCC. DU145 cells were cultivated in RPMI-1640 growth

[1]Department of Internal Medicine I and Comprehensive Cancer Center, Medical University of Vienna, Vienna, Austria. [2]Department of Surgery and Core Facility Flow Cytometry, Medical University of Vienna, Vienna, Austria. [3]Clinical Institute of Pathology, Medical University of Vienna, Vienna, Austria.

Note: Supplementary data for this article are available at Molecular Cancer Research Online (http://mcr.aacrjournals.org/).

E. Tomasich and A. El-Gazzar contributed equally to this article.

Corresponding Author: Peter Horak, Department of Internal Medicine I and Comprehensive Cancer Center, Medical University of Vienna, Waehringer Guertel 18-20, A-1090 Vienna, Austria. Phone: 43-1-40400-73792; Fax: 43-1-40400-1685; E-mail: peter.horak@meduniwien.ac.at

doi: 10.1158/1541-7786.MCR-14-0153-T

AACR

medium enriched with 10% FCS, whereas TRAMP-C1 cells were grown in DMEM with 4 mmol/L L-glutamine, 5 μg/mL insulin, 10 nmol/L DHT, 5% FBS, and 5% Nu Serum (BD Biosciences). Both media were supplemented with 50 units/mL penicillin G and 50 μg/mL streptomycin sulfate, and cells were grown at 37°C in a humidified atmosphere with 5% CO_2 and 3% O_2. Selective HIF1 inhibitor blocking the hypoxia-induced accumulation of cellular HIF1α protein was used (CAS 934593-90-5; Merck Millipore).

Lentiviral transduction and transfection

Downregulation of HIF1α in the DU145 prostate cancer cell line was performed by lentiviral delivery using pLKO.1 vector containing HIF1α shRNA (Open Biosystems, Thermo Fisher Scientific) and HEK293T packaging cell line. Transduced cells were selected and maintained in medium containing puromycin (3 μg/mL).

Breeding of transgenic TRAMP mice and tumor isolation

Male C57BL/6-Tg(TRAMP)8247 Ng/J mice hemizygous for the *PB-TAg* transgene were generated by mating transgenic adenocarcinoma of the mouse prostate (TRAMP) hemizygous females with nontransgenic C57BL/6 males. The TRAMP transgene was identified using DNA extracted from tail samples following the genotyping protocol provided by the Jackson Laboratory. The animal experiments described within this study were approved by the Animal Ethics Committee of the Medical University of Vienna (Vienna, Austria). Prostates from male mice (25–44 weeks old) were isolated using forceps and scalpel and dissociated into single-cell suspensions using the Papain Dissociation System according to the manufacturer's protocol (LK003150; Worthington Biochemical Corp.).

Prostate cancer xenograft tumor models

Eight-week-old male NSG JAX (NOD.Cg-*Prkdc*^{scid} *Il2rg*^{tm1Wjl}/SzJ) mice were purchased from Charles River Laboratories and injected subcutaneously with indicated numbers of DU145 cells in 100 μL PBS and Matrigel (BD Biosciences) mixed 1:1 using a 25G needle. Growth was monitored weekly and measured in 2 dimensions using a caliper. Tumor volume was calculated using the formula $V = 4/3 \times \pi \times (\text{length}/2) \times (\text{width}/2)^2$. Mice were sacrificed once the tumors reached a critical size set by the Animal Ethics Committee of the Medical University of Vienna.

FACS and analysis

CSCs and CSC-like cells were analyzed in murine primary TRAMP tumors, TRAMP-C1 cell line and human DU145 prostate cancer cell line using FACS (BD FACSAria I, Becton Dickinson or MoFlo Astrios) according to their expression of known stem cell markers (ref. 24; Lin$^-$/Sca-1$^+$/CD49f$^+$ for primary TRAMP cells, Sca-1$^+$/CD49f$^+$ for the murine TRAMP-C1 cell line, and CD49f$^+$/CD44$^+$ for human DU145 cell line). The LIVE/DEAD fixable yellow dead cell stain kit (L34959, Invitrogen) was used for viability discrimination. In absence of distinct subpopulations in the two cell line models (TRAMP-C1 and DU145), we sorted 15% of cells with the highest and lowest expression of both markers, respectively. For intracellular staining, cells were fixed with paraformaldehyde and cell membranes were permeabilized using digitonin solution. Following this step, cell suspensions were incubated with primary antibodies against pS6, S6, pAkt, and Akt overnight at 4°C. On the next day, the cells were incubated with a secondary fluorescent antibody for 1 hour at room temperature and analyzed using the MoFlo Astrios System. For used antibodies, please refer to Supplementary Table S1. Compensations for multicolor analyses were set using Anti-Mouse IgG, κ/Negative Control compensation Particle Set (Becton Dickinson), Anti-Rat and Anti-Hamster IgG,κ/Negative Control compensation Particle Set (Becton Dickinson), and ArC Amine Reactive compensation Bead Kit (Invitrogen) labeled with appropriate antibodies and concentrations. Analysis of results was performed using the FlowJo software (TreeStar Inc.).

Isolated CSCs from the DU145 and murine TRAMP-C1 cell line were further cultured in their respective growth media as described above at 37°C in a humidified atmosphere with 5% CO_2 and 3% O_2. Unless otherwise stated, hypoxic conditions (3% O_2) were chosen for subculturing of sorted CSC and non-CSC populations from DU145 and TRAMP-C1 cell lines to preserve and enhance their stem cell-like properties (25, 26). Cells were subcultured in hypoxia (3% oxygen) for not longer than 4 days. All experiments were performed within 72 hours from plating. To ensure replicable conditions for our *in vitro* experiments and prevent a possible loss of phenotype, we performed a FACS of same passage TRAMP-C1 and DU145 cells before each batch of experiments.

Apoptosis assay

Using 6-well plates, DU145 control (scrCo) and DU145 HIF1-knockdown (shHIF1A) cells were incubated in hypoxia (3% O_2) for 72 hours. Cells were harvested together with the supernatant and washed in PBS with 2% FBS. Cells were then stained for CD44 and CD49f as described above. In the next step, cells were incubated with AnnexinV-APC and 7-aminoactinomycin D (7-AAD) fluorescent dies (#550474 and #559925, BD Biosciences) for 15 minutes in the dark at 4°C, resuspended and analyzed using a BD LSRFortressa flow cytometer. Analysis of results was performed using the FlowJo software.

Spheroid formation assays

Using 24-well plates, 2,500 cells per well were cultivated in triplicate wells in serum-free RPMI-1640 (DU145) or DMEM (TRAMP-C1) medium and 50% Matrigel (BD Biosciences) for 10 days. Medium was changed every second day. Counting of spheres with a diameter more than 50 μm was done after fixing the cells in 10% formalin and staining with crystal violet.

Protein isolation and immunoblotting

Cells were lysed using the RIPA buffer supplemented with Complete Protease Inhibitor Cocktail Tablets (Roche Diagnostics) and PhosSTOP Phosphatase Inhibitor Cocktail Tablets (Roche Diagnostics). After incubation for 10 minutes on ice, cell lysates were cleared by centrifugation at 15,000 rpm for 10 minutes at 4°C and protein concentration of the supernatant was determined by Bradford absorbance assay (Sigma-Aldrich). Equal amounts of protein (30 μg) were separated by SDS-PAGE, blotted on polyvinylidene difluoride (PVDF) membranes (GE Healthcare), incubated with appropriate primary antibodies, and visualized via horseradish peroxidase (HRP)-conjugated secondary antibodies and the ECL chemiluminescent detection system (GE Healthcare). The following antibodies and dilutions were used: primary antibodies against pS6-Ser240/244 [#2215] (1:1,000),

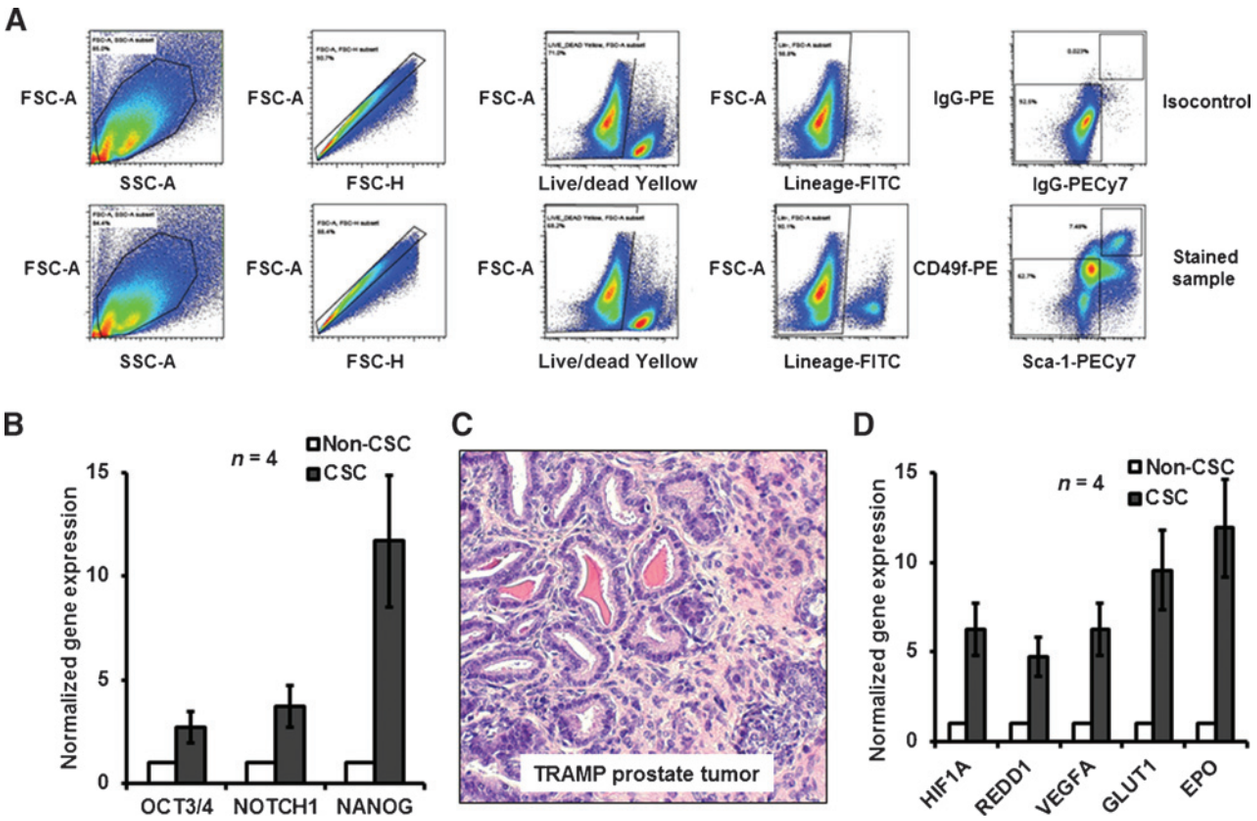

Figure 1.
A, analysis of prostate CSCs in primary TRAMP tumors. FACS gating strategy to identify the Lin$^-$/CD49f$^+$/Sca-1$^+$ population in primary TRAMP tumors. A distinct subpopulation of TRAMP tumors cells could be identified (bottom row, last graph). Only live single-cell populations were used for analysis. Appropriate isotype control antibodies (top row) were used as negative controls. B, TRAMP CSCs express increased mRNA levels of *Notch1, Oct3/4*, and *Nanog* ($n = 4$). C, hematoxylin and eosin staining of a representative TRAMP tumor section (40× magnification). D, HIF target gene mRNA upregulation in TRAMP tumors. mRNA was isolated from sorted Lin$^-$/CD49f$^+$/Sca-1$^+$ (CSC) and Lin$^-$/CD49f$^-$/Sca-1$^-$ (non-CSC) subpopulations. *Vegfa, Glut1, Pdk1, Redd1*, and *Epo* mRNA were significantly upregulated in CSCs relative to non-CSCs using qRT-PCR. *Hif1α* mRNA was also upregulated 6-fold in TRAMP CSCs ($n = 4$).

S6 [#2217] (1:1,000), pAkt-Ser473 [#4060] (1:1,000), Akt [#9272] (1:1,000), pIRS-1-Ser302 [#2384] (1:300), IRS-1 [#2390] (1:300), PTEN [#9552] (1:1,000) from Cell Signaling Technology; AR [sc-116] (1:1,000), β-actin [sc-1616 (1:1,000) and HRP-conjugated secondary antibodies (donkey anti-goat [sc-2020] (1:10,000), donkey anti-rabbit [sc-2077] (1:10,000) from Santa Cruz Laboratories. Quantification of Western blot analyses was performed using the public domain ImageJ software (developed at U.S. NIH, Bethesda, MD).

Immunoprecipitation and immunoblotting

Cells were lysed in immunoprecipitation (IP) lysis buffer (PBS with 0.75% NP-40, complete Protease Inhibitor Cocktail Tablets and PhosSTOP Phosphatase Inhibitor Cocktail Tablets) and Bradford assay was performed to determine protein concentrations. Two micrograms of HIF1α antibody [Novus Biologicals (NB100-105)] were added to 500 μg of the protein sample and incubated for 90 minutes at 4°C followed by incubation with protein G/protein A sepharose beads (GE Healthcare) overnight. Consequently, beads were washed 3 times in the IP lysis buffer, and SDS-PAGE and Western blotting were performed as described above. Antibodies and dilutions used for Western blot analysis: anti- HIF1α [(MAB1536), 1:500; R&D Systems] and goat anti-mouse IgG-HRP [(sc-2005), 1:10,000; Santa Cruz Laboratories].

Cell viability assays

Ten thousand cells per well were plated in 96-well plates in triplicates and cultured in 100 μL medium per well as described above with different concentrations of sirolimus (Selleck Biochem) as indicated for up to 72 hours. Cell viability was assessed by adding 10 μL of Cell Titer Blue reagent (Promega) to each well and subsequent measurement of the absorbance at 570 and 600 nm (as reference) after 4 to 6 hours using a Berthold TriStar LB 941 Multimode Microplate Reader (Berthold Technologies).

RNA isolation, cDNA synthesis, and qRT-PCR

Total RNA was prepared with RNAzol RT (Molecular Research Center Inc.) and quantified with a NanoDrop 8000 spectrophotometer (Thermo Scientific). cDNA was created using the SuperScript Double-Stranded cDNA Synthesis Kit (Invitrogen). For quantitative HIF1α analysis, TaqMan Gene Expression Assays by Applied Biosystems with murine and human HIF1α probes (Mm00468869_m1 and Hs00153153_m1) and 18S ribosomal RNA as controls (Mm03928990_g1 and Hs03928990_g1) were

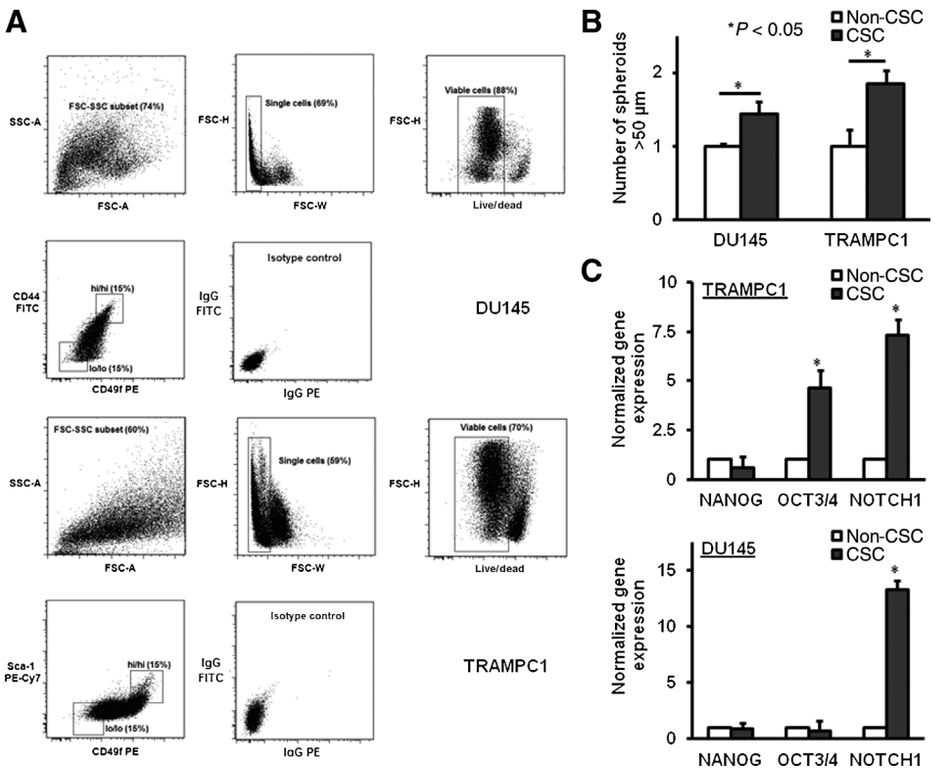

Figure 2.
A, isolation of CSC-like cells from DU145 and TRAMP-C1 cell lines. FACS gating strategy to identify and sort the CSC-like subpopulations in the DU145 (top 5 graphs) and TRAMP-C1 (bottom 5 graphs) cell lines. In each cell line, the 15% of cells with highest fluorescent signal (hi/hi, $CD44^+$ /$CD49f^+$ for DU145, $CD49f^+$/$Sca\text{-}1^+$ for TRAMP-C1, respectively) and 15% of cells with lowest fluorescent signal (lo/lo) were isolated. Viability staining and doublet discrimination as well as isotype control antibodies (isotype control) were used. B, number of spheroids larger than 50 µm and normalized to non-CSC count after 10 days in 50% Matrigel and serum-free medium. Means and SDs of triplicate experiments are shown. C, mRNA expression of *NANOG*, *OCT3/4*, and *NOTCH1* in sorted prostate CSC-like cells (CSC) of human (DU145) and murine (TRAMP-C1) origin, compared with non–CSC-like (non CSC) cells (normalized to 1). *, $P < 0.05$.

used. Power SYBRGreen (Applied Biosystems)-based qRT-PCR reactions were performed for *NOTCH1*, *NANOG*, *OCT3/4*, *GLUT1*, *PDK1*, *VEGF-A*, *REDD1*, *EPO*, and 18S rRNA using primers designed with the Primer3 software (Supplementary Table S3). Analysis was done on a StepOnePlus RT-PCR System (Applied Biosystems), and gene expression was normalized to human or murine 18S rRNA.

Results

Identification of a basal prostate CSC subpopulation in TRAMP mice

The TRAMP mouse model has been recently used to study prostate CSCs and their tumorigenicity *in vivo* (27). We evaluated 24 prostate samples from male TRAMP mice at different stages of tumor development and identified a distinct Lin^-/$Sca\text{-}1^+$/$CD49f^+$ (cancer) stem cell subpopulation in 19 animals (82.61%, Supplementary Fig. S2A). This $Sca\text{-}1^+$/$CD49f^+$ CSC subpopulation constituted on average 2.97% of the total Lin^- cell population (Fig. 1A and Supplementary Table S2). We confirmed the histologic phenotype of prostate adenocarcinoma in selected tumors (Fig. 1C), as neuroendocrine prostate cancer may also arise in this model. Interestingly, basal HIF1α mRNA levels were elevated several fold in prostate CSCs compared with non-CSCs from TRAMP mice (Fig. 1D). We could also observe transcriptional HIF1α upregulation in murine basal prostate stem cells (Lin^-/$Sca\text{-}1^+$/$CD49f^+$) from age-matched wild-type C57BL/6 mice (Supplementary Fig. S1A), suggesting upregulation of hypoxic signaling in normal as well as tumor-derived murine prostate stem cells. We measured mRNA expression of known HIF targets to analyze and confirm hypoxia-induced downstream signaling in these cells and found elevated levels of *Glut1*, *Epo*, and *Vegfa* mRNA (Fig. 1D). Furthermore, Redd1, a hypoxic regulator of mTOR activity and a HIF1α target, was upregulated in CSCs from TRAMP tumors. mRNA expression of *Nanog* and *Oct3/4*, two pluripotency-associated transcription factors involved in stem cell self renewal and maintenance, as well as *Notch1* were increased in TRAMP-derived prostate CSCs, thus additionally supporting a CSC phenotype (Fig. 1B).

To corroborate our findings, we isolated CSC-like cells from TRAMP-C1 cell line, which was derived from a TRAMP prostate adenocarcinoma. First, we characterized and profiled the TRAMP-C1 cell line using known basal stem cell markers (CD44, CD49f, Sca-1, and Trop-2) and isolated CSC-like cells by means of $Sca\text{-}1^+$/$CD49f^+$ surface expression corresponding to the phenotype of primary TRAMP cells (Fig. 2A). Furthermore, we profiled and isolated CSC-like cells from the PTEN-positive, androgen-independent human prostate cancer cell line DU145 using the expression of the human basal stem cell markers CD44 and CD49f (Fig. 2A). To confirm the CSC properties of the sorted double-positive cells, we performed *in vitro* sphere formation assays (as surrogate readout of stemness) as well as mRNA expression analysis of stem cell function and differentiation-associated genes, such as *NOTCH1*, *OCT3/4*, and *NANOG*. Isolated CSC-like cells from both cell lines demonstrated increased sphere formation capability (Fig. 2B) and significant upregulation of *OCT3/4* and/or *NOTCH1* (Fig. 2C).

HIF signaling is elevated in prostate CSC-like cells

Hypoxic conditions are known to promote stemness and self-renewal of CSCs (28–31). Increased HIF1α mRNA levels in TRAMP-derived prostate cancer cells led us to analyze the hypoxic response of CSC-like cells in the cell culture model. We could demonstrate that mRNA expression of HIF target genes (human

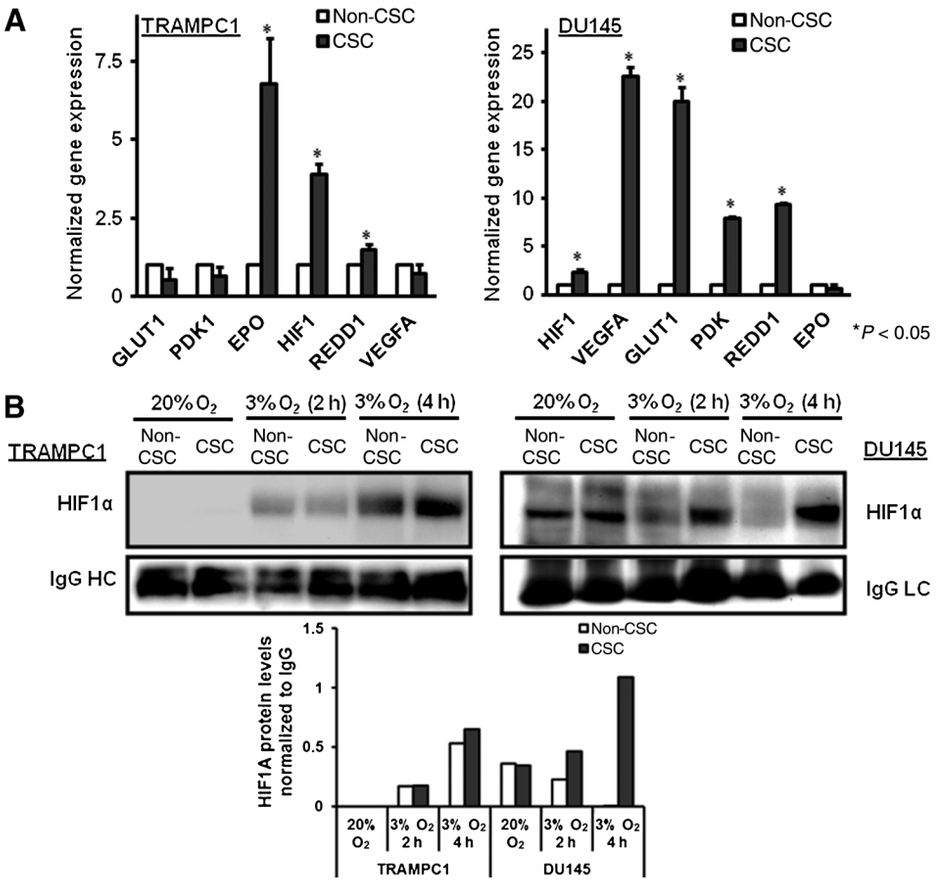

Figure 3.
A, HIF target gene mRNA upregulation in prostate CSC-like cells (CSC). Sorted cell populations were subjected to 72 hours hypoxia (3% O_2) and evaluated for expression of *HIF1α, VEGF-A, GLUT1, PDK1, REDD1*, and *EPO. Hif1α* as well as *Epo* and *Redd1* were significantly upregulated in hypoxic murine (TRAMPC1) CSC-like cells. The human (DU145) CSC-like cells show elevated mRNA expression of *VEGF-A, GLUT1, PDK1*, and *REDD1* in comparison to non-CSCs. Error bars show SD. *, $P < 0.05$. B, HIF1α is preferentially stabilized in the TRAMP-C1 and DU145-derived CSC-like cells after 2 and 4 hours of hypoxia. After sorting, cells were cultured under normoxic (20% O_2) conditions for 24 hours and subjected to hypoxia for the specified intervals. HIF1α protein levels were assessed by IP and Western blotting. IgG heavy chain (HC) or light chain (LC) is shown as a loading control for IP. Quantification of HIF1α protein expression relative to the loading control is shown below.

and murine *GLUT1*, *REDD1*, *PDK1*, *VEGF-A*, and *EPO*) in hypoxia is consistently higher in human and murine prostate CSC-like cells (Fig. 3A). Because HIF1α is regulated primarily by protein stabilization under hypoxic conditions, we evaluated protein levels of HIF1α in CSC-like cells in hypoxia. For this experiment, we cultured TRAMP-C1- and DU145-derived CSC-like cells for 48 hours at ambient oxygen levels and subjected them to short-term hypoxia (4 hours, 3% O_2). HIF1α stabilization and expression is induced more prominently in CSC-like cells from both prostate cancer cell lines in a time-dependent manner (Fig. 3B), although we observed marked differences between the two cell lines. Surprisingly, DU145-derived $CD44^-/CD49f^-$ cells did not display HIF1α expression within the first 4 hours of hypoxia (Fig. 3B).

HIF1α inhibits mTOR and activates AKT phosphorylation in prostate CSC-like cells

CSCs are thought of as slowly proliferating, multipotent, and consequently chemo- and radiotherapy-resistant cells. To study the effects of hypoxia on mTOR and AKT signaling, two key regulators of cellular growth and proliferation, we further cultivated isolated CSC-like cells under hypoxic conditions for up to 72 hours. We could indeed demonstrate elevated AKT activity, assessed by serine 473 phosphorylation, in prostate CSC-like cells (Fig. 4A). Next, we investigated mTOR activity by analyzing its downstream effects on S6 phosphorylation. Hypoxic regulation of mTOR signaling in hypoxia has been well-described (19). Indeed, mTOR activity of CSC-like cells was markedly decreased in hypoxia (Fig. 4A), thus suggesting a hypoxic inhibition of mTOR despite AKT activation. To assess possible reciprocal feedback regulations of PI3K pathway and androgen receptor (AR) signaling, we evaluated PTEN and AR expression. No significant differences in PTEN and AR expression between CSC-like and non–CSC-like cells in the two cell lines were observed (Fig. 4A). We also demonstrated a relative decrease in S6 phosphorylation accompanied by an increase in Akt phosphorylation (Fig. 5B) in CSCs from primary TRAMP tumors, which validated our findings in primary cells. This effect on AKT and S6 phosphorylation could not be observed under normoxic conditions (Fig. 4B). To confirm that HIF1α was indeed responsible for the S6 dephosphorylation and AKT activation in hypoxic CSC-like cells, we knocked down the expression of HIF1α in the DU145 and TRAMP-C1 cell lines (Supplementary Fig. S1C and S1D). The shHIF1A-transduced CSC-like cells display attenuation of AKT phosphorylation and simultaneous increase in S6 phosphorylation in hypoxia (Fig. 4C), thus reversing the aforementioned effect and indicating an HIF1α-dependent mechanism. In addition, we treated the DU145 cells with a specific HIF1α inhibitor, which led to a reduction of HIF1α protein levels (Supplementary Fig. S1B). This selective HIF1α inhibition also results in a decline of hypoxic AKT activation (Fig. 4D). These results prompted us to analyze the known feedback loops regulating the PI3K/AKT/mTOR axis. Hence we analyzed the feedback regulation of PI3K through S6K-

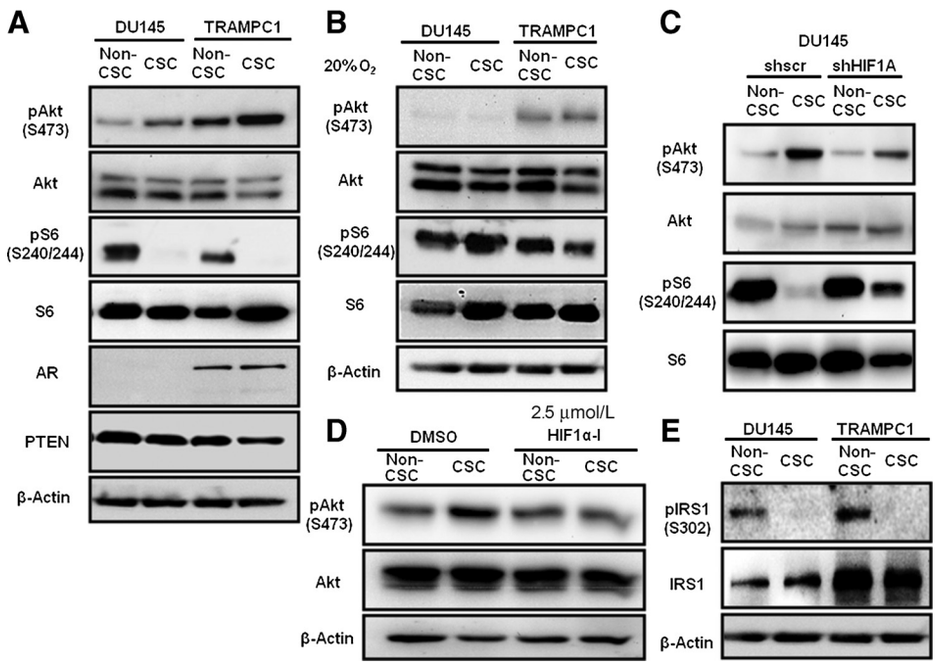

Figure 4.

A, increased phosphorylation of AKT at Ser473 and decreased phosphorylation of S6 at Ser240/244 in CSC-like cells (CSC) isolated from the DU145 and TRAMP-C1 cell lines. AR and PTEN expression remained unchanged between the CSC and non CSC cells. β-Actin served as loading control. B, cells were cultured in normoxia (20% O_2) for 72 hours before lysis. Under these conditions, CSC-like cells did not display a deregulation of AKT or S6 phosphorylation levels, suggesting no significant differences in mTOR signaling. C, shRNA-mediated knockdown of HIF1α (shHIF1A) in the DU145 cell line leads to a reduction of the effects on S6 and AKT phosphorylation in hypoxic CSC-like cells. Scrambled shRNA (scrCo) served as control. D, treatment with 2.5 μmol/L HIF1α inhibitor leads to a reduction of feedback phosphorylation of Akt Ser473 in TRAMP-C1 CSC-like cells. Cells were treated for 72 hours in hypoxia (3% O_2) with the HIF1α inhibitor or DMSO. Relative quantification of Western blot bands is provided in Supplementary Fig. S3. E, feedback phosphorylation of IRS-1 is reduced in CSC-like cells. Ser302 (murine sequence) or Ser307 (human sequence) phosphorylation of IRS-1 as a measure of feedback inhibition by S6K1 is decreased in CSC-like cells in both cell lines.

mediated IRS-1 phosphorylation as a possible explanation for the observed effects. Indeed, we could determine significant dephosphorylation of IRS-1 as a result of S6K inactivation in prostate CSC-like cells (Fig. 4E), suggesting a feedback activation of AKT through IRS-1 in CSC-like cells in hypoxia.

Knockdown of HIF1α in prostate CSC-like cells increases their viability in hypoxia

We demonstrated decreased mTOR signaling in response to hypoxia in prostate CSCs. Consequently, we were curious how HIF1α loss might affect proliferation, apoptosis, and viability of prostate CSCs. Upon HIF1α knockdown, human as well as murine prostate CSC-like cells seem to gain a growth advantage over their non-CSC counterparts (Fig. 5A). We could not attribute this effect to changes in apoptosis, although we see an increase in viable cell fractions in the CSC-like subpopulation (Supplementary Fig. S2B). In addition, we injected 8-week-old male NSG mice subcutaneously with HIF1α downregulated and sorted DU145 non-CSC and CSC populations. Here, we observed an enhanced engraftment and growth of the CSC subpopulation in controls as well as tumors with downregulated HIF (Supplementary Fig. S4B and S4C), which was further augmented upon HIF1α knockdown (Fig. 5C). No significant differences in xenograft growth were observed between scrambled shRNA-transduced cells and wild-type DU145 cells (Supplementary Fig. S4A).

Prostate CSCs have previously been shown to be sensitive to dual PI3K/mTOR inhibitors (32). Given the profound alterations of mTOR signaling in hypoxic CSC-like cells, we were curious whether they still remained sensitive to mTOR inhibition. We evaluated the viability of sorted cell populations after treatment with rapamycin (sirolimus). In general, we found that prostate CSC-like cells in hypoxia were more resistant to rapamycin than their non–CSC-like counterparts (Fig. 5A). Our results suggest that prostate CSCs, which demonstrate decreased mTOR activity and proliferation under conditions of chronic hypoxia, are more resistant to selective mTOR inhibition.

Discussion

CSCs are thought to be the main force behind tumor initiation, progression, and metastasis and the successful targeting and elimination of CSCs are the foundations of an effective cancer therapy. However, the origin of distinct prostate CSCs remains a moot point (6, 7, 33). The TRAMP mouse model represents an extensively characterized SV40 T-antigen–driven mouse model of prostatic adenocarcinoma (27, 34), and we used well-established markers to isolate murine prostate (cancer) stem cells of basal origin in this model (24, 35). We show that by FACS of TRAMP prostates using published protocols, we can successfully isolate and analyze a CSC subpopulation in TRAMP mice. However, a possible disadvantage of this model is the inherent heterogeneity of the developing

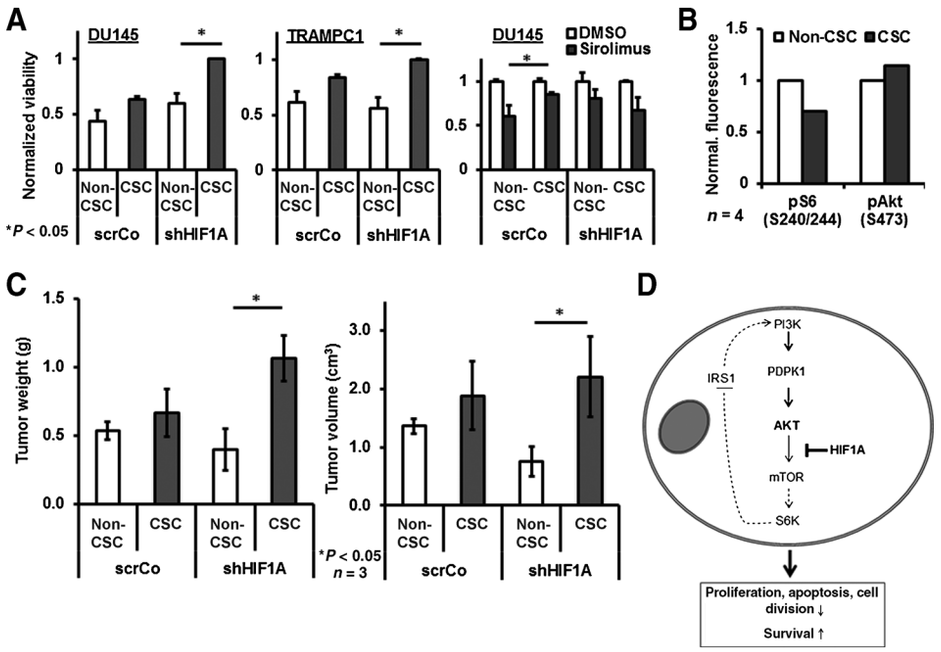

Figure 5.
A, HIF1α downregulation leads to increased proliferation of prostate CSCs in hypoxia. HIF1α shRNA (shHIF1A) and scrambled shRNA control (scrCo) were lentivirally transduced into DU145 and TRAMP-C1 cells. Prostate CSCs show resistance to mTOR inhibitors, which can be reversed by HIF1α loss. HIF1α shRNA (shHIF1A) and scrambled RNA control were lentivirally transduced into DU145 cells. Sorted CSC-like cells were plated in 96-well plates, allowed to adhere overnight, and grown for additional 72 hours at 3% O_2 or treated with a 100 nmol/L concentration of mTOR inhibitor rapamycin (sirolimus) or DMSO. Means and SDs relative to DMSO-treated cells of 3 independent experiments are shown. B, fluorescent intracellular staining and analysis of phosphorylated S6 and Akt in primary TRAMP tumor cells. Decrease in S6 phosphorylation and a small increase in Akt phosphorylation, recapitulating the regulatory mechanism observed in cell culture was observed. Amount of phosphorylation is depicted as relative to total S6 and Akt protein and normalized to 1. C, three male 8-week-old NSG mice were injected in 4 ventral subcutaneous sites with 1×10^5 sorted CSC and non-CSC subpopulations of shHIF1A as well as sorted control (scrCo) DU145 cells, respectively. Tumor size was measured regularly and mean tumor volume and weight at the time of sacrifice are shown. Error bars indicate SEM. *, $P < 0.05$. D, proposed hypoxic feedback regulation in prostate CSCs. In contrast to non-CSCs, prostate CSCs have increased HIF mRNA and protein levels resulting in mTOR inhibition and feedback activation of AKT. As a consequence, CSCs exhibit lower growth and proliferation rates under hypoxic conditions, which might lead to their increased maintenance and survival.

tumors arising through unregulated viral transformation. Although TRAMP mice develop a higher percentage of neuroendocrine tumors under certain conditions (in the FVB background, or following castration; ref. 36), we histologically confirmed the presence of early-stage prostatic intraepithelial neoplasia as well as prostatic adenocarcinoma (late stage) in the dissected animals. However, the issue of intertumoral heterogeneity remains, which might explain our failure to isolate basal prostate CSC subpopulations from all TRAMP tumor specimens.

PTEN, as a master regulator of the PI3K/AKT/mTOR axis, plays an important role in prostate cancer progression. Its function in prostate (cancer) stem cells is less well documented, partly due to the use of PTEN-driven prostate cancer models (37–39). PTEN loss has been shown to constitute a late event in prostate carcinogenesis (40, 41). Loss of PTEN function might thus not be essential for human prostate CSC development and/or maintenance. Our results in PTEN-expressing prostate cancer models suggest that constitutive expression of PTEN and its inhibitory effects on PI3K signaling may be required for homeostasis in a subset of prostate CSCs.

In our work, we emphasize the role of differential HIF1α expression in epithelial prostate stem cells as well as prostate cancer–initiating cells. Expression of HIF1α has been implicated as an oncogenic factor for prostate cancer development (42) and hypoxic signaling through HIF seems to be regulating prostate CSC properties (29) as well as metastasis (18). HIF upregulation in cancer can occur under normoxic as well as hypoxic conditions and has been well documented (31). Under normoxic conditions, HIF levels are tightly regulated by prolyl hydroxylation and subsequent proteasomal degradation. However, HIF overexpression in cancer cells may not depend on the physiologic, post-translational regulation. In fact, transcriptional regulation of HIF1α by heat shock factors, NF-κB, angiotensin II, and other mechanisms has been described (43–46). Increased HIF1α levels have been observed in primary prostate cancer (47), but the degree and significance of HIF1α expression in prostate CSCs have been unknown. We suggest that HIF1α upregulation might lead to mTOR inhibition and a regulatory feedback activation of AKT specifically in prostate CSCs (Fig. 5D). Negative regulation of mTOR in response to hypoxia is primarily mediated through expression of REDD1 (19) and might offer an explanation for our observations. REDD1, due to its transcriptional regulation by TP63 as well as HIF1α, is a bona fide candidate for this type of interaction in basal prostate CSCs (48). We could show that prostate CSCs require HIF1α to control their proliferation and promote their survival in hypoxia. Attenuation of mTOR signaling in CSCs through the hypoxia-inducible factor may thus lead not only to metabolic adaptation through anaerobic glycolysis and angiogenesis but also to (cancer) stem cell maintenance (28, 29, 31). In consequence, prostate CSCs may be dependent on

mTOR deactivation to strive in the hypoxic tumor microenvironment, as has been observed in HSCs (49). This may lead to an intrinsic resistance of prostate CSCs to mTOR inhibitors and a possible explanation for their lack of efficacy in clinical trials (50). We believe that inhibition of several different kinases along the PTEN/AKT/mTOR axis and/or HIF1α may be required for efficient pharmaceutical targeting of prostate CSCs.

To summarize, we observe transcriptional upregulation of HIF1α in prostate (cancer) stem cells through a yet unidentified mechanism, which might in turn lead to elevated hypoxic signaling in CSCs, leading to their survival in the hypoxic niche. We also suggest that decreased mTOR activity in response to HIF1α upregulation inhibits proliferation and promotes survival of prostate CSCs through the IRS-1/PI3K feedback loop.

Disclosure of Potential Conflicts of Interest

No potential conflicts of interest were disclosed.

Authors' Contributions

Conception and design: M. Marhold, M. Krainer, P. Horak
Development of methodology: M. Marhold, E. Tomasich, A. El-Gazzar, A. Spittler, P. Horak
Acquisition of data (provided animals, acquired and managed patients, provided facilities, etc.): M. Marhold, E. Tomasich, A. El-Gazzar, G. Heller, A. Spittler, R. Horvat
Analysis and interpretation of data (e.g., statistical analysis, biostatistics, computational analysis): M. Marhold, A. El-Gazzar, A. Spittler, R. Horvat, M. Krainer, P. Horak
Writing, review, and/or revision of the manuscript: M. Marhold, A. Spittler, M. Krainer, P. Horak
Administrative, technical, or material support (i.e., reporting or organizing data, constructing databases): E. Tomasich, G. Heller, R. Horvat
Study supervision: M. Krainer, P. Horak

Acknowledgments

The authors thank Andrea Schanzer, Maria König, Günther Hofbauer, Corinna Altenberger, Barbara Ziegler, and Sonja Reynoso de Leon for expert technical assistance and collegiality.

Grant Support

This work was supported by the Vienna Fund for Innovative Interdisciplinary Cancer Research, Initiative Krebsforschung Grant to P. Horak; OeGHO Dissertation Grant for Translational Research in Medical Oncology to M. Marhold, Research Grant of the Fellinger Krebsforschung to M. Marhold, and Centre for International Cooperation and Mobility of the Austrian Agency for International Cooperation in Education and Research (Project no. CZ 04/2012).

The costs of publication of this article were defrayed in part by the payment of page charges. This article must therefore be hereby marked *advertisement* in accordance with 18 U.S.C. Section 1734 solely to indicate this fact.

Received March 20, 2014; revised October 8, 2014; accepted October 10, 2014; published OnlineFirst October 27, 2014.

References

1. Dick JE. Stem cell concepts renew cancer research. Blood 2008;112:4793–807.
2. Domingo-Domenech J, Vidal SJ, Rodriguez-Bravo V, Castillo-Martin M, Quinn SA, Rodriguez-Barrueco R, et al. Suppression of acquired docetaxel resistance in prostate cancer through depletion of notch- and hedgehog-dependent tumor-initiating cells. Cancer Cell 2012;22:373–88.
3. Goldstein AS, Huang J, Guo C, Garraway IP, Witte ON. Identification of a cell of origin for human prostate cancer. Science 2010;329:568–71.
4. Wang X, Kruithof-de Julio M, Economides KD, Walker D, Yu H, Halili MV, et al. A luminal epithelial stem cell that is a cell of origin for prostate cancer. Nature 2009;461:495–500.
5. Wang ZA, Mitrofanova A, Bergren SK, Abate-Shen C, Cardiff RD, Califano A, et al. Lineage analysis of basal epithelial cells reveals their unexpected plasticity and supports a cell-of-origin model for prostate cancer heterogeneity. Nat Cell Biol 2013;15:274–83.
6. Wang ZA, Shen MM. Revisiting the concept of cancer stem cells in prostate cancer. Oncogene 2011;30:1261–71.
7. Stoyanova T, Cooper AR, Drake JM, Liu X, Armstrong AJ, Pienta KJ, et al. Prostate cancer originating in basal cells progresses to adenocarcinoma propagated by luminal-like cells. Proc Natl Acad Sci U S A 2013;110:20111–6.
8. Choi N, Zhang B, Zhang L, Ittmann M, Xin L. Adult murine prostate basal and luminal cells are self-sustained lineages that can both serve as targets for prostate cancer initiation. Cancer Cell 2012;21:253–65.
9. Collins AT, Berry PA, Hyde C, Stower MJ, Maitland NJ. Prospective identification of tumorigenic prostate cancer stem cells. Cancer Res 2005;65:10946–51.
10. Goldstein AS, Lawson DA, Cheng D, Sun W, Garraway IP, Witte ON. Trop2 identifies a subpopulation of murine and human prostate basal cells with stem cell characteristics. Proc Natl Acad Sci U S A 2008;105:20882–7.
11. Richardson GD, Robson CN, Lang SH, Neal DE, Maitland NJ, Collins AT. CD133, a novel marker for human prostatic epithelial stem cells. J Cell Sci 2004;117:3539–45.
12. Burger PE, Xiong X, Coetzee S, Salm SN, Moscatelli D, Goto K, et al. Sca-1 expression identifies stem cells in the proximal region of prostatic ducts with high capacity to reconstitute prostatic tissue. Proc Natl Acad Sci U S A 2005;102:7180–5.
13. Lawson DA, Xin L, Lukacs RU, Cheng D, Witte ON. Isolation and functional characterization of murine prostate stem cells. Proc Natl Acad Sci U S A 2007;104:181–6.
14. Xin L, Lawson DA, Witte ON. The Sca-1 cell surface marker enriches for a prostate-regenerating cell subpopulation that can initiate prostate tumorigenesis. Proc Natl Acad Sci U S A 2005;102:6942–7.
15. Goldstein AS, Stoyanova T, Witte ON. Primitive origins of prostate cancer: *in vivo* evidence for prostate-regenerating cells and prostate cancer-initiating cells. Mol Oncol 2010;4:385–96.
16. Takubo K, Goda N, Yamada W, Iriuchishima H, Ikeda E, Kubota Y, et al. Regulation of the HIF-1alpha level is essential for hematopoietic stem cells. Cell Stem Cell 2010;7:391–402.
17. Shiozawa Y, Pedersen EA, Havens AM, Jung Y, Mishra A, Joseph J, et al. Human prostate cancer metastases target the hematopoietic stem cell niche to establish footholds in mouse bone marrow. J Clin Invest 2011;121:1298–312.
18. Mishra A, Wang J, Shiozawa Y, McGee S, Kim J, Jung Y, et al. Hypoxia stabilizes GAS6/Axl signaling in metastatic prostate cancer. Mol Cancer Res 2012;10:703–12.
19. DeYoung MP, Horak P, Sofer A, Sgroi D, Ellisen LW. Hypoxia regulates TSC1/2-mTOR signaling and tumor suppression through REDD1-mediated 14-3-3 shuttling. Genes Dev 2008;22:239–51.
20. Laplante M, Sabatini DM. mTOR signaling in growth control and disease. Cell 2012;149:274–93.
21. Sansal I, Sellers WR. The biology and clinical relevance of the PTEN tumor suppressor pathway. J Clin Oncol 2004;22:2954–63.
22. Baselga J, Campone M, Piccart M, Burris HA III, Rugo HS, Sahmoud T, et al. Everolimus in postmenopausal hormone-receptor-positive advanced breast cancer. N Engl J Med 2012 366:520–9.
23. Hudes G, Carducci M, Tomczak P, Dutcher J, Figlin R, Kapoor A, et al. Temsirolimus, interferon alfa, or both for advanced renal-cell carcinoma. N Engl J Med 2007;356:2271–81.
24. Lukacs RU, Goldstein AS, Lawson DA, Cheng D, Witte ON. Isolation, cultivation and characterization of adult murine prostate stem cells. Nat Protoc 2010 5:702–13.
25. Ivanovic Z. Hypoxia or in situ normoxia: the stem cell paradigm. J Cell Physiol 2009;219:271–5.

26. McCord AM, Jamal M, Shankavaram UT, Lang FF, Camphausen K, Tofilon PJ. Physiologic oxygen concentration enhances the stem-like properties of CD133+ human glioblastoma cells *in vitro*. Mol Cancer Res 2009;7: 489–97.
27. Mazzoleni S, Jachetti E, Morosini S, Grioni M, Piras IS, Pala M, et al. Gene signatures distinguish stage-specific prostate cancer stem cells isolated from transgenic adenocarcinoma of the mouse prostate lesions and predict the malignancy of human tumors. Stem Cells Transl Med 2013;2:678–89.
28. Li Z, Bao S, Wu Q, Wang H, Eyler C, Sathornsumetee S, et al. Hypoxia-inducible factors regulate tumorigenic capacity of glioma stem cells. Cancer Cell 2009;15:501–13.
29. Ma Y, Liang D, Liu J, Axcrona K, Kvalheim G, Stokke T, et al. Prostate cancer cell lines under hypoxia exhibit greater stem-like properties. PLoS One 2012;6:e29170.
30. Seidel S, Garvalov BK, Wirta V, von Stechow L, Schanzer A, Meletis K, et al. A hypoxic niche regulates glioblastoma stem cells through hypoxia inducible factor 2 alpha. Brain 2010;133:983–95.
31. Mimeault M, Batra SK. Hypoxia-inducing factors as master regulators of stemness properties and altered metabolism of cancer- and metastasis-initiating cells. J Cell Mol Med 2013;17:30–54.
32. Dubrovska A, Elliott J, Salamone RJ, Kim S, Aimone LJ, Walker JR, et al. Combination therapy targeting both tumor-initiating and differentiated cell populations in prostate carcinoma. Clin Cancer Res 2010;16:5692–702.
33. Li Y, Laterra J. Cancer stem cells: distinct entities or dynamically regulated phenotypes? Cancer Res 2012;72:576–80.
34. Greenberg NM, DeMayo F, Finegold MJ, Medina D, Tilley WD, Aspinall JO, et al. Prostate cancer in a transgenic mouse. Proc Natl Acad Sci U S A 1995;92:3439–43.
35. Mulholland DJ, Xin L, Morim A, Lawson D, Witte O, Wu H. Lin-Sca-1+CD49fhigh stem/progenitors are tumor-initiating cells in the Pten-null prostate cancer model. Cancer Res 2009;69:8555–62.
36. Tang Y, Wang L, Goloubeva O, Khan MA, Lee D, Hussain A. The relationship of neuroendocrine carcinomas to anti-tumor therapies in TRAMP mice. Prostate 2009;69:1763–73.
37. Di Cristofano A, De Acetis M, Koff A, Cordon-Cardo C, Pandolfi PP. Pten and p27KIP1 cooperate in prostate cancer tumor suppression in the mouse. Nat Genet 2001;27:222–4.
38. Kim MJ, Cardiff RD, Desai N, Banach-Petrosky WA, Parsons R, Shen MM, et al. Cooperativity of Nkx3.1 and Pten loss of function in a mouse model of prostate carcinogenesis. Proc Natl Acad Sci U S A 2002;99:2884–9.
39. Wang S, Gao J, Lei Q, Rozengurt N, Pritchard C, Jiao J, et al. Prostate-specific deletion of the murine Pten tumor suppressor gene leads to metastatic prostate cancer. Cancer Cell 2003;4:209–21.
40. Feilotter HE, Nagai MA, Boag AH, Eng C, Mulligan LM. Analysis of PTEN and the 10q23 region in primary prostate carcinomas. Oncogene 1998; 16:1743–8.
41. McMenamin ME, Soung P, Perera S, Kaplan I, Loda M, Sellers WR. Loss of PTEN expression in paraffin-embedded primary prostate cancer correlates with high Gleason score and advanced stage. Cancer Res 1999;59:4291–6.
42. Kimbro KS, Simons JW. Hypoxia-inducible factor-1 in human breast and prostate cancer. Endocr Relat Cancer 2006;13:739–49.
43. Chen R, Liliental JE, Kowalski PE, Lu Q, Cohen SN. Regulation of transcription of hypoxia-inducible factor-1alpha (HIF-1alpha) by heat shock factors HSF2 and HSF4. Oncogene 2011;30: 2570–80.
44. Nardinocchi L, Puca R, Guidolin D, Belloni AS, Bossi G, Michiels C, et al. Transcriptional regulation of hypoxia-inducible factor 1alpha by HIPK2 suggests a novel mechanism to restrain tumor growth. Biochim Biophys Acta 2009;1793:368–77.
45. Page EL, Robitaille GA, Pouyssegur J, Richard DE. Induction of hypoxia-inducible factor-1alpha by transcriptional and translational mechanisms. J Biol Chem 2002;277:48403–9.
46. Rius J, Guma M, Schachtrup C, Akassoglou K, Zinkernagel AS, Nizet V, et al. NF-kappaB links innate immunity to the hypoxic response through transcriptional regulation of HIF-1alpha. Nature 2008;453: 807–11.
47. Zhong H, Semenza GL, Simons JW, De Marzo AM. Up-regulation of hypoxia-inducible factor 1alpha is an early event in prostate carcinogenesis. Cancer Detect Prev 2004;28:88–93.
48. Ellisen LW, Ramsayer KD, Johannessen CM, Yang A, Beppu H, Minda K, et al. REDD1, a developmentally regulated transcriptional target of p63 and p53, links p63 to regulation of reactive oxygen species. Mol Cell 2002;10: 995–1005.
49. Huang J, Nguyen-McCarty M, Hexner EO, Danet-Desnoyers G, Klein PS. Maintenance of hematopoietic stem cells through regulation of Wnt and mTOR pathways. Nat Med 2012;18:1778–85.
50. Templeton AJ, Dutoit V, Cathomas R, Rothermundt C, Bartschi D, Droge C, et al. Phase 2 trial of single-agent everolimus in chemotherapy-naive patients with castration-resistant prostate cancer (SAKK 08/08). Eur Urol 2012;64:150–8.